

An Application of Three-Dimensional Finite Element Method to Thawing Processes in Foodstuffs

Hidemasa MIKI*, Hiroyuki KIKUKAWA** and Jun-ichi NISHIMOTO*

Abstract

The three-dimensional finite element method was applied to the analysis of thawing processes of "kamaboko", which was used as a homogeneous foodstuff. In order to check the program, beforehand, comparisons of numerical solutions with existing analytical solutions were made for heating of a finite cylinder without phase-change on various time steps. The numerical solutions were in good agreement with the analytical solutions when an adequate time step was chosen, and yielded good approximations for the experimental results in the frozen zone below the melting point. However, for more agreement in the melted zone, the interpolation of heat capacity and thermal conductivity at the narrow temperature range above and below the melting point, in which the phase-change takes place abruptly, may be necessary. And for practical applications, time step, grid size, boundary conditions and material variations have to be more carefully estimated.

The finite element method was first proposed for field problems by O. C. ZIENKIEWICZ and Y. K. CHEUNG¹⁾²⁾. Since then many researchers have published books and reports on the fundamental concept and various applications of this method on the heat conduction¹⁾⁻⁷⁾. Recently, G. COMINI et al.¹⁾ reported applications of the method to computation of temperature curves in foodstuffs of irregular shape during freezing and thawing with phase-change. MIKI et al.⁴⁾ described applications of this method to thawing processes in frozen fish. Most authors have discussed only one- or two-dimensional geometries. And for practical problems, three-dimensional problem with irregular shape should be considered. Therefore, this study is undertaken to extend the applications of the finite element method to the solution of a transient heat transfer problem during thawing in three-dimensional geometries of foodstuffs. Evaluations of thermal properties in foodstuffs and time step are also discussed.

Physical Aspects

When foodstuffs are cooled below the freezing point (T_f), which is considered to be equal to the melting point or the thawing point in the present paper, a ratio (ξ) of ice to total water at a temperature (T) is represented approximately by⁸⁾:

* Laboratory of Food Preservation Science, Faculty of Fisheries, Kagoshima University, Japan

** Laboratory of Engineering Oceanography, Faculty of Fisheries, Kagoshima University, Japan

$$\xi = 1 - \frac{T_f}{T}. \quad (1)$$

The specific heat (c_f) of water in foodstuffs below the freezing point has been defined by GENSYO⁹⁾ as:

$$c_f = c_1 + (c_1 - c_2) \frac{T_f}{T} - \lambda_w \frac{T_f}{T^2}. \quad (2)$$

In the phase-change zone, a straight line can be used to interpolate the specific heat (c_f) of water including the latent heat effect as shown in Fig. 1¹⁰⁾. As is seen from Eq. (2), c_f is expressed for a function of temperature (T) in the phase-change zone.

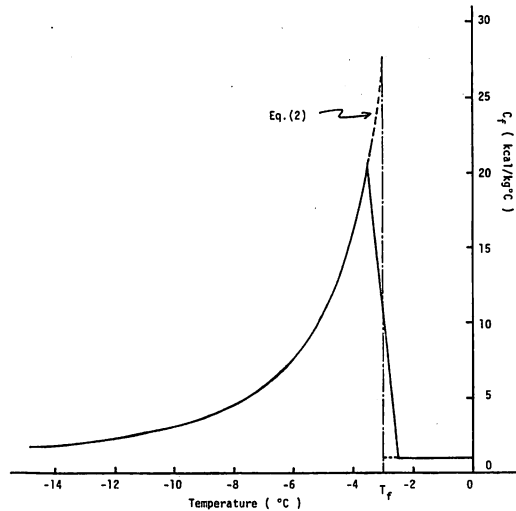


Fig. 1. Specific heat of water around the melting point is approximated by the solid line instead of the dashed line (Eq. (2)).

New estimations of density and thermal conductivity of homogeneous foodstuffs above and below the freezing point have been proposed by YANO¹¹⁾ as following equations:

i) Density (ρ) of foodstuffs¹¹⁾:

$$\rho = \frac{1}{X/\rho_w + Y/\rho_l + (1-X-Y)/\rho_d}, \quad (3)$$

where X , Y and $(1-X-Y)$ are mass fractions of water, lipid and solid (protein, carbohydrate) in foodstuffs. The values of ρ_w , ρ_l and ρ_d indicate densities of water, lipid and solid. These values above 0°C and at -10°C are shown in Table 1¹¹⁾.

ii) Specific heat (c) of foodstuffs¹²⁾:

$$c = c_w X + c_l Y + c_d (1 - X - Y), \quad (4)$$

where c_w , c_l and c_d represent specific heat of water, lipid and solid. These values above 0°C and -10°C are shown in Table 2¹¹⁾.

Table 1. Densities of each constituent in foodstuffs.

	above 0°C^{**}	-10°C^{***}
ρ_w	1000 [kg/m ³]	918 [kg/m ³]
ρ_d	1300 "	1300 "
ρ_l	900* "	930* "

* Measured by YANO.¹¹⁾

** Used above T_f [$^\circ\text{C}$] in the present paper.

*** Used below T_f [$^\circ\text{C}$] in the present paper.

Table 2. Specific heats of each constituent in foodstuffs.

	above 0°C^{**}	-10°C^{***}
c_w	1.0 [kcal/kg $^\circ\text{C}$]	0.48 [kcal/kg $^\circ\text{C}$]
c_d	0.3 "	0.30 "
c_l	0.5 "	0.37* "

* Measured by YANO.¹¹⁾

** Used above T_f [$^\circ\text{C}$] in the present paper.

*** Used below T_f [$^\circ\text{C}$] in the present paper.

iii) Thermal conductivity (k) of foodstuffs:

Effective thermal conductivity of heterogeneous system has been expressed as¹¹⁾:

$$k = \frac{1}{X^v/k_w + Y^v/k_l + (1-X-Y)^v/k_d}, \quad (5)$$

here

$$X^v = \frac{X/\rho_w}{X/\rho_w + Y/\rho_l + (1-X-Y)/\rho_d}, \quad (6)$$

$$Y^v = \frac{Y/\rho_l}{X/\rho_w + Y/\rho_l + (1-X-Y)/\rho_d}, \quad (7)$$

$$(1-X-Y)^v = \frac{(1-X-Y)/\rho_d}{X/\rho_w + Y/\rho_l + (1-X-Y)/\rho_d}, \quad (8)$$

where X^v , Y^v and $(1-X-Y)^v$ are volume fraction of water, lipid and solid.

Provided $T \leq T_f$, the values of ρ_w , c_w and k_w in Eqs. (3)–(5) are replaced as follows⁴⁾:

$$\rho_w = (1-\xi)\rho_1 + \xi\rho_2, \quad (9)$$

$$c_w = c_f, \quad (10)$$

$$k_w = (1-\xi)k_1 + \xi k_2, \quad (11)$$

where subscripts 1 and 2 express water and ice respectively in Eqs. (2), (9) and (11). These values above and below the freezing point (T_f) are shown in Tables 1 to 3. Thermal properties of the chief constituents in foodstuffs are shown in Table 3⁽¹⁰⁾. Provided $T > T_f$, the values of c_w , ρ_w and k_w are equal to the each physical property of water in liquid.

Table 3. Thermal conductivities of the chief constituent in foodstuffs.

	k [kcal/mh°C]
water	2.0
ice	
liquid	0.48
Solid	
(protein,	0.26 (0°C)*?
carbohydrate)	0.42 (-10°C)
Lipid	0.12-0.15**

* Used 0.42 [kcal/mh°C] in the present paper.

** Used 0.15 [kcal/mh°C] in the present paper.

Experimental

Sample

“Kamaboko” was used as a homogeneous and commercially available foodstuff. The samples of kamaboko manufactured by Nakashin Kamaboko Honten LTD. (Kushikino-shi), with net weight of 290 g, were obtained at a local supermarket. These samples were made from rinsed muscles of Alaska pollack (*Theraga chalcogramma*), Lizardfish (*Saurida undosquamis*) and other's additions, i.e., salt, starch, sugar, polyphosphate, etc. .

Thawing procedure

The samples were first equilibrated at -18°C and -72°C . The frozen sample of -18°C was thawed at room temperature of 21°C . The other frozen sample of -72°C was thawed at room temperature of 19°C . Thermocouples (Cu-Con., 0.3 mm ϕ) for measurement of temperatures were inserted into the samples as shown in Fig. 4 before freezing, and then thawing curves were recorded by the automatic temperature recorder (Yokogawa Elec. Works LTD., ER-4036).

Constituent analysis

Water content (X) was determined by the infrared watermeter (Kett Elec. Laboratory LTD., F-1A). Lipid content (Y) is assumed as 0.01 in the present paper. Solid content ($1 - X - Y$) was calculated from the measured values X and Y .

Formulation

In this section we give the finite element formulation for the three dimensional heat conduction. As in Ref. 4, we assume the isotropic heat conduction coefficient. Then the governing equation is given as follows:

$$\rho c \frac{\partial T}{\partial t} - k \left(\frac{\partial^2 T}{\partial x^2} + \frac{\partial^2 T}{\partial y^2} + \frac{\partial^2 T}{\partial z^2} \right) = 0 \quad (12)$$

with the boundary condition:

$$k \left(\frac{\partial T}{\partial x} n_x + \frac{\partial T}{\partial y} n_y + \frac{\partial T}{\partial z} n_z \right) + \alpha (T - T_a) = 0, \quad (13)$$

(on the boundary S)

where ρ is the density, c the specific heat, k the isotropic thermal conductivity, n_x , n_y and n_z the direction cosines of the outward normal to the boundary surface, α the convective heat transfer coefficient and T_a is the temperature of the atmosphere.

We divide the three dimensional domain into hexahedrons. This division makes the numbering of nodal point easier than that of direct division into tetrahedral elements. One hexahedral element is further divided into five tetrahedral subelements by two ways shown in Fig. 2²⁾. A 8×8 hexahedral element stiffness matrix is given by summing ten 4×4 subelement stiffness matrices of tetrahedrons. The averaging of the two ways of subdivision makes our computational scheme more stable.

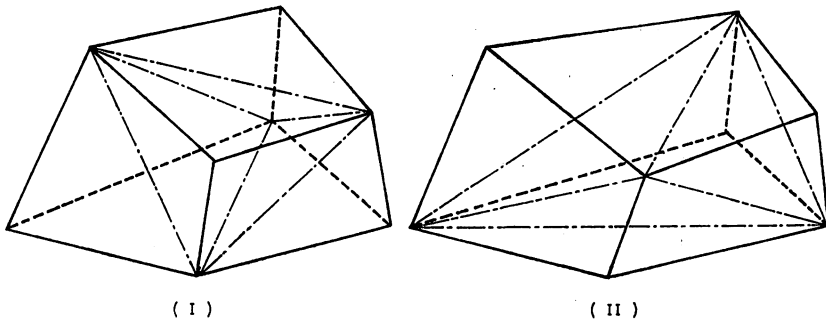


Fig. 2. A hexahedral element is divided by five tetrahedral subelements in two ways.²⁾

As in Ref. 4, we consider the functional for one tetrahedral subelement,

$$\begin{aligned} \delta \mathcal{X}_{sub}^e &= \int_{\Omega} T^* \left\{ \rho c \frac{\partial T}{\partial t} - k \left(\frac{\partial^2 T}{\partial x^2} + \frac{\partial^2 T}{\partial y^2} + \frac{\partial^2 T}{\partial z^2} \right) \right\} dv \\ &= \int_{\Omega} \left\{ T^* \rho c \frac{\partial T}{\partial t} + k \left(\frac{\partial T^*}{\partial x} \frac{\partial T}{\partial x} + \frac{\partial T^*}{\partial y} \frac{\partial T}{\partial y} + \frac{\partial T^*}{\partial z} \frac{\partial T}{\partial z} \right) \right\} dv \\ &\quad + \alpha \int_S T^* (T - T_a) dA, \end{aligned} \quad (14)$$

where T^* is the weighting function and dv and dA denote the three and two dimensional integrations respectively. Ω is the domain of a tetrahedral subelement and S is its surface on the boundary. Following the GALERKIN's method we write T and T^* by,

$$T = L_i T_i, \quad T^* = L_i T_i^* \quad (i=1-4) \quad (15)$$

where L_i denote the volume coordinates and T_i and T_i^* represent the temperatures and their variations at the four vertices of the tetrahedron. For completeness we give the volume coordinates L_i .

$$L_i = \frac{1}{6v}(a_i + b_i x + c_i y + d_i z), \quad (16)$$

$$a_i = A_{1i}, \quad b_i = A_{2i}, \quad c_i = A_{3i}, \quad d_i = A_{4i}, \quad (i=1-4) \quad (17)$$

where v is the volume of the tetrahedral subelement and A_{ij} are the cofactors of the element of the following determinant:

$$\begin{vmatrix} 1 & 1 & 1 & 1 \\ x_1 & x_2 & x_3 & x_4 \\ y_1 & y_2 & y_3 & y_4 \\ z_1 & z_2 & z_3 & z_4 \end{vmatrix} \quad (18)$$

In Eq. (18) (x_i, y_i, z_i) are the values of the coordinates at the i -th vertex of the tetrahedron.

The time derivative in Eq. (14) is approximated by,

$$\frac{\partial T}{\partial t} = L_i \frac{T_i(t) - T_i(t - \Delta t)}{\Delta t}. \quad (19)$$

Then the functional is rewritten as:

$$\begin{aligned} \delta \mathcal{X}_{sub}^e = T_i^* \left\{ \left[k(M^x + M^y + M^z) + \frac{\rho c}{\Delta t} M + \alpha B \right]_{ij} T_j(t) \right. \\ \left. - \frac{\rho c}{\Delta t} (M)_{ij} T_j(t - \Delta t) + \alpha (B_a)_i \right\}, \quad (20) \end{aligned}$$

where

$$\begin{aligned} (M)_{ij} &= \int_{\Omega} L_i L_j dv, & (M^x)_{ij} &= \int_{\Omega} \frac{\partial L_i}{\partial x} \frac{\partial L_j}{\partial x} dv, \\ (M^y)_{ij} &= \int_{\Omega} \frac{\partial L_i}{\partial y} \frac{\partial L_j}{\partial y} dv, & (M^z)_{ij} &= \int_{\Omega} \frac{\partial L_i}{\partial z} \frac{\partial L_j}{\partial z} dv, \\ (B)_{ij} &= \int_S L_i L_j dA, & (B_a)_i &= \int_S T_a L_i dA. \end{aligned} \quad (21)$$

The integrals of Eq. (21) can be easily performed by using the formulas¹²⁾:

$$\int_v L_1^a L_2^b L_3^c L_4^d dv = \frac{a!b!c!d!}{(a+b+c+d+3)!} 6v,$$

$$\int_S L_1^a L_2^b L_3^c dA = \frac{a!b!c!}{(a+b+c+2)!} 2A. \quad (22)$$

The variational functional of one hexahedral element is given by summing ten functionals of tetrahedral subelement:

$$\delta x^e = \frac{1}{2} \left\{ \sum_{sub(1)} \delta x_{sub(1)}^e + \sum_{sub(2)} \delta x_{sub(2)}^e \right\}.$$

And the variational functional for the whole domain is the sum of all the functionals of hexahedral elements:

$$\delta x = \sum_e \delta x^e$$

Requiring that δx is equal to zero for any variations T_i^* ($i=1-N$, N is the number of the nodal points of the whole domain), a matrix equation follows by which we can determine the temperatures $T_i(t)$ if $T_i(t-\Delta t)$ are known.

Computational Results

Comparison with analytical solution

In order to see the reliability of our numerical method, we will compare the computational results with the analytical solution. Considering a column, we use the analytical solution:

$$T = T_a + (T_0 - T_a) \exp \left\{ -\frac{kt}{R^2 \rho c} \left[\mu^2 + \left(\frac{R}{H} \right)^2 \nu^2 \right] \right\} J_0 \left(\frac{\mu r}{R} \right) \cos \left(\frac{\nu z}{H} \right), \quad (23)$$

where r and z are column coordinates, R and H are radius and the height of the column respectively, J_0 is the 0-th order Bessel function and the constants μ and ν are determined by the following equations:

$$\frac{\mu J_1(\mu)}{J_0(\mu)} = \frac{\alpha R}{k}, \quad (24)$$

$$\frac{\nu \sin(\nu)}{\cos(\nu)} = \frac{\alpha H}{k}. \quad (25)$$

We take for instance, the following values for the constants:

$$\rho c = 1.0 \text{ kcal/m}^3 \text{ } ^\circ\text{C},$$

$$k = 0.25 \text{ kcal/mh } ^\circ\text{C}, \quad \alpha = 37.5 \text{ kcal/m}^2 \text{h } ^\circ\text{C}$$

$$H=2.0 \text{ cm}, \quad R=2.0 \text{ cm},$$

$$T_0=4.0 \text{ }^\circ\text{C}, \quad T_a=35.0 \text{ }^\circ\text{C}.$$

Then from Eqs. (24) and (25) μ and ν are determined to be:

$$\mu=\sqrt{3.19}, \quad \nu=1.193.$$

We have plotted Eq. (23) by the solid curve in Fig. 3.

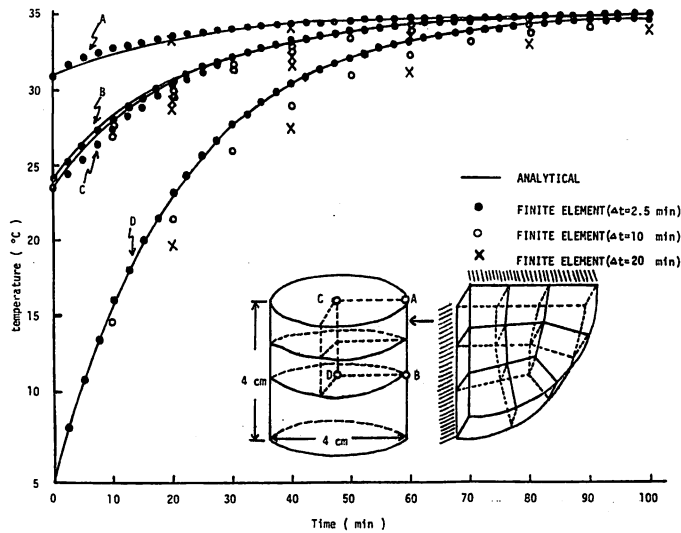


Fig. 3. Comparison of numerical solutions with the analytical ones.

The numerical calculation was carried out by dividing the column using the hexahedral elements also shown in Fig. 3. The numerical results are given by the dots in the figure. For the time step Δt equal to 2.5 minutes, the agreement with the analytical solution is wonderful, but if Δt increases the computational results tend to go lower than the analytical solution. If we take much smaller time step, the computation comes to be unstable. Thus we will take 2.5 minutes for the time step if the similar hexahedral elements shown in Fig. 3 are used. The favorable time step depends on the volumes of the hexahedrons and physical parameters such as thermal conductivity. If we divide the space into smaller pieces, the favorable time step might become small.

Comparison with experimental result

We have applied our numerical scheme to the thawing process of kamaboko. The division of kamaboko into hexahedral elements are shown in Fig. 4. As the elements have similar volumes as those in Fig. 3, the time step is chosen to be 2.5 minutes. We have used the physical parameters given in Tables 1-3. The con-

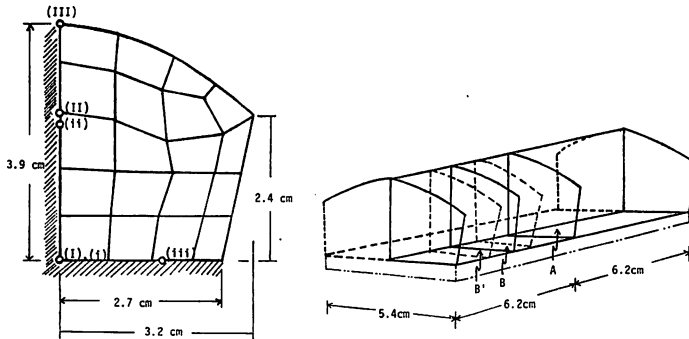


Fig. 4. Our division of kamaboko into hexahedral elements. Dashed lines represent the boundary and our numerical results are written at the surfaces of A and B'. The number of the hexahedral elements is $19 \times 3 = 57$. While experiments are performed at the surfaces A and B.

vective heat transfer coefficients are 24 and 20 ($\text{Kcal}/\text{m}^2\text{h}^\circ\text{C}$) for the thawing processes with initial temperatures -18 and -72 ($^\circ\text{C}$) respectively. These values are natural if the natural convections are induced.

The experimental results are shown in Figs. 5 and 6, and the numerical results are shown in Figs. 7 and 8. The agreement with the experimental results may be re-

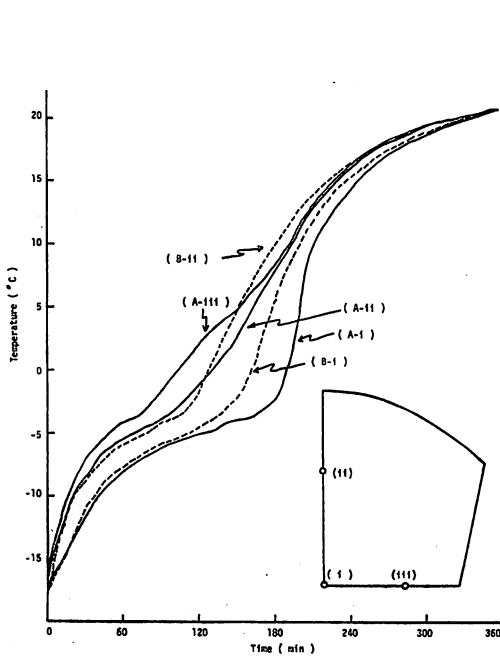


Fig. 5. Experimental results at the surfaces A and B when the initial temperature is -18°C .

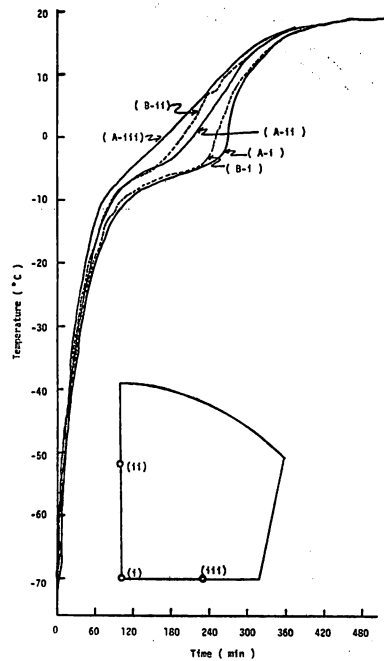


Fig. 6. Experimental results at the surfaces A and B when the initial temperature is -72°C ,

spectable. Especially the three dimensional effects have been rightly estimated. We hope the agreement to increase if the parameters are more carefully chosen.

As can be seen in Figs. 7 and 8, the numerical results show a little unstable features. The unstability increases if we use Eq. (2) instead of our practical one shown in Fig. 1 for the specific heat of water. In order to obtain more stable results, all the physical parameters have to be made perfectly smooth.

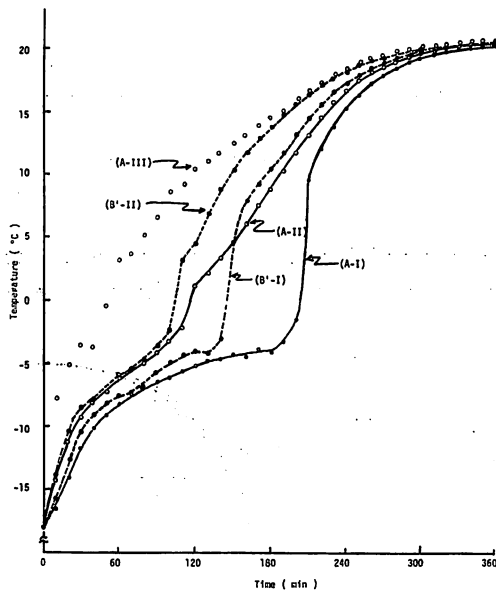


Fig. 7. Numerical solutions at the surfaces A and B' when the initial temperature is -18°C . I, II, III are given in Fig. 4.

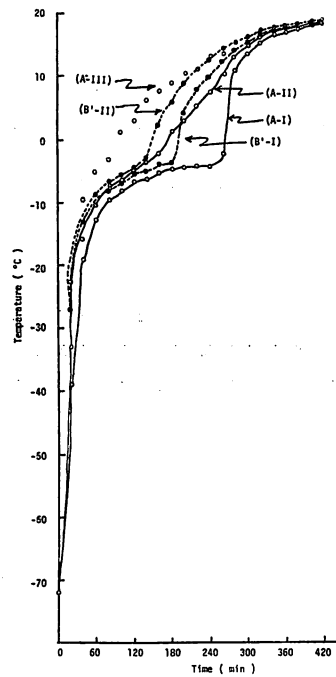


Fig. 8. Numerical solutions at the surfaces A and B' when the initial temperature is -72°C . I, II, III are given in Fig. 4.

Discussion

Disagreements between the numerical and experimental results in the melted zone above the melting point ($=T_m$) are probably due to poor approximation of thermal properties. The thermal conductivity of dry solid above the melting point was assumed $c_d=0.42$, which was equal to the value of -10°C , to obtain a better fit. On the estimation of thermal properties of foodstuffs, it was assumed that YANO's equations¹¹⁾ gave almost the same effect to computed results as TANAKA's equations¹³⁾ used in the previous report⁴⁾.

For more agreement, it is necessary to estimate thermal properties of biological materials with accuracy and interpolate heat capacity (c_p) and thermal conductivity

(k) at the phase-change zone close to the melting point. And for practical problems, time step, grid size, boundary conditions and material variations have to be more carefully treated.

In general, it may be considered that three dimensional finite element method can be used to simulate the thawing processes of foodstuffs having irregular cubic shapes. This analogy may be extended for prediction of deterioration and evaluation of stress cracks which will occur in foodstuffs during freezing and thawing processes. Furthermore, this method can be applied for solution of mass diffusion in foodstuffs on the processing problems of preservation such as drying, smoking and salting etc. .

Acknowledgements

Authors wish to thank Prof. Fuyuo OHTA and Prof. Sadato ISHIBASHI, Kagoshima University, for many helpful suggestions to our study. Furthermore, we would like to express our special appreciation to Prof. Danji NOMURA and Assoc. Prof. Isao HAYAKAWA, Kyushu University, for their encouragement. The computation was carried out in FACOM M-200 of Computer Center of Kyushu University.

Notations

- c = Specific heat (kcal/kg°C)
 n_x, n_y, n_z = Direction cosines of the outward normal to the boundary surface
 N = Number of the nodal points
 q = Heat capacity (kcal/kg)
 S = Boundary surface
 T = Temperature (°C)
 X = Mass fraction of water
 Y = Mass fraction of lipid
 $1-X-Y$ = Mass fraction of dry solid
 α = Convective heat transfer coefficient (kcal/m²h°C)
 λ = Latent heat (kcal/kg)
 ξ = Ratio of ice to total water in foods
 ρ = Density (kg/m³)
 χ = Functional of the variational principle
 Ω = Domain of a tetrahedral subelement

Subscripts and superscripts

- | | |
|----------------------|--|
| a = Ambient | v = volume fraction |
| d = Dry solid | w = Water |
| e = Element | x, y, z = In the x, y, z direction |
| f = Freezing point | 1 = water in liquid |
| l = Lipid | 2 = Ice |

References

- 1) G. COMINI, S. DEL GUIDICE, R. W. LEWIS and O. C. ZIENKIEWICZ: *Int. J. Num. Meth. Engng.*, **8**, 613-624 (1974).
O. C. ZIENKIEWICZ and Y. K. CHUNG: *The Engineer*, **220**, 507-510 (1965).
- 2) O. C. ZIENKIEWICZ: *The Finite Element Method*, 3rd ed., McGraw-Hill, London, 1977.
- 3) L. J. SEGERLIND: *Applied Finite Element Analysis*, 1st ed., John Wiley Sons, New York, 1976.
- 4) H. MIKI, H. KIKUKAWA and J. NISHIMOTO: *Mem. Fac. Fish., Kagoshima Univ.*, **27**, 107-115 (1978).
- 5) L. REBELLATO, S. DELGIUDICE and G. COMINI: *J. Food Sci.*, **43**, 239-243 (1978).
- 6) R. N. MISRA and J. H. YOUNG: *Trans. of the ASME*, 944-949 (1979).
- 7) G. E. MYERS: *Trans. of ASME*, **100**, 120-127 (1978).
- 8) I. GENSHO: *Refrigeration*, **12**, 12-19 (1937). (In Japanese)
- 9) I. GENSHO: *ibid.*, **45**, 8-15 (1970). (In Japanese)
- 10) C. BONACINA, G. COMINI, A. FASANO and M. PRIMICERIO: *Int. J. Heat Mass Trans.*, **18**, 861-867 (1974).
- 11) T. YANO: *New Food Industry*, **20**, 55-73 (1979). (In Japanese)
- 12) M. A. EISENBERG and E. M. LAWRENCE: *Int. J. Num. Meth. Engng.*, **7**, 574-575 (1973).
- 13) K. TANAKA and T. KOJIMA: *Food Refrigeration Engineering*, 1st ed., Koseisya Koseikaku, Tokyo, 1976, 142-145. (In Japanese)